Mol Neurobiol (2017) 54:2301–2312
DOI 10.1007/s12035-016-9824-3

Adenosine Monophosphate-Activated Protein Kinase Abates Hyperglycaemia-Induced Neuronal Injury in Experimental Models of Diabetic Neuropathy: Effects on Mitochondrial Biogenesis, Autophagy and Neuroinflammation

Veera Ganesh Yerra[1] · **Ashutosh Kumar**[1]

Received: 12 January 2016 / Accepted: 2 March 2016 / Published online: 8 March 2016

Abstract Impaired adenosine monophosphate kinase (AMPK) signalling under hyperglycaemic conditions is known to cause mitochondrial dysfunction in diabetic sensory neurons. Facilitation of AMPK signalling is previously reported to ameliorate inflammation and induce autophagic response in various complications related to diabetes. The present study assesses the role of AMPK activation on mitochondrial biogenesis, autophagy and neuroinflammation in experimental diabetic neuropathy (DN) using an AMPK activator (A769662). A769662 (15 and 30 mg/kg, i.p) was administered to Sprague–Dawley rats (250–270 g) for 2 weeks after 6 weeks of streptozotocin (STZ) injection (55 mg/kg, i.p.). Behavioural parameters (mechanical/thermal hyperalgesia) and functional characteristics (motor/sensory nerve conduction velocities (MNCV and SNCV) and sciatic nerve blood flow (NBF)) were assessed. For in vitro studies, Neuro2a (N2A) cells were incubated with 25 mM glucose to simulate high glucose condition and then studied for mitochondrial dysfunction and protein expression changes. STZ administration resulted in significant hyperglycaemia (>250 mg/dl) in rats. A769662 treatment significantly improved mechanical/thermal hyperalgesia threshold and enhanced MNCV, SNCV and NBF in diabetic animals. A769662 exposure normalised the mitochondrial superoxide production, membrane depolarisation and markedly increased neurite outgrowth of N2A cells. Further, AMPK activation also abolished the NF-κB-mediated neuroinflammation. A769662 treatment increased Thr-172 phosphorylation of AMPK results in stimulated PGC-1α-directed mitochondrial biogenesis and autophagy induction. Our study supports that compromised AMPK signalling in hyperglycaemic conditions causes defective mitochondrial biogenesis ultimately leading to neuronal dysfunction and associated deficits in DN and activation of AMPK can be developed as an attractive therapeutic strategy for the management of DN.

Keywords AMPK · Autophagy · Diabetic neuropathy · Mitochondrial dysfunction · Neuroinflammation · PGC-1α

Introduction

Microvascular complications of diabetes imposes major health burden in developed as well as developing countries [1]. Diabetic neuropathy (DN) has very high prevalence (50–60 %) in subjects with chronic diabetes [2]. Altered axonal transmission, increased pain sensitisation, abnormal sensations and allodynia are common symptoms associated with DN [3]. Aetiopathogenesis of DN is least characterised and is reported to be mediated through enhanced generation of reactive oxygen species (ROS), improper bioenergetic supply, amplified apoptosis, loss of insulinotropic support, nuclear factor kappa B (NF-κB)-directed neuroinflammation, inefficient removal of damaged proteins and organelles in neurons and glial cells [4–6]. These interwoven pathways further complicates the therapeutic targeting for the management of DN. Duloxetine and pregabalin are the only FDA-approved drugs for the palliative care in DN [7]. Non-uniform success, limited options and the need for an ideal therapeutic intervention necessitates further research in the area of DN [8].

Neurons meet high metabolic demands for growth and neurotransmission from oxidative phosphorylation [9]. Hence,

✉ Ashutosh Kumar
ashutosh.niperhyd@gov.in; ashutoshniper@gmail.com

[1] Department of Pharmacology and Toxicology, National Institute of Pharmaceutical Education and Research (NIPER), Balanagar, Hyderabad, TG 500037, India

failure of mitochondrial function in neurons may lead to neuropathological consequences such as impaired growth, metabolism and disturbed neurotransmission. Hyperglycaemia-directed silencing of adenosine monophosphate kinase (AMPK) leads to mitochondrial dysfunction which can contribute to vascular complications of diabetes [10]. AMPK activation adds to ATP generation by enhancing catabolic cellular pathways, increasing mitochondrial function and by removing damaged mitochondria through mitophagy [11]. Mitochondrial biogenesis through peroxisome proliferator-activated receptor-gamma coactivator 1 alpha (PGC-1α) has been reported to ameliorate several chronic diseases associated with mitochondrial dysfunction [12]. Active biogenesis of mitochondria should be complemented with efficient removal of damaged mitochondria by active autophagy process which is essential for maintaining cellular and redox homeostasis [13]. Mitochondrial dysfunction and altered bioenergetics have been known to exert their pathological footprints in sensory deficits in streptozotocin (STZ)-induced diabetes [14, 15]. However, the pharmacological benefit of activating the mitochondrial biogenesis and autophagy through modulation of bioenergetic sensor, AMPK, in experimental DN is an unexplored avenue.

We evaluated the pharmacological potential of AMPK activation in terms of regulation of mitochondrial function and their turnover in experimental models of DN using A769662, an allosteric activator of AMPK [16]. A769662 has been documented for its potential effect on AMPK activation in several experimental models including those of neuropathic pain [17]. We have studied the ROS generation, mitochondrial superoxide generation and neurite outgrowth in N2A cells to characterise the effect of AMPK signalling facilitation on mitochondrial performance and neuronal growth. The effect of A769662 on neuroinflammation, PGC-1α mediated mitochondrial biogenesis and autophagy induction was studied in in vitro and in vivo models of experimental DN.

Materials and Methods

Animals

Healthy male Sprague–Dawley rats (250–270 g) were fed on standard diet and water ad libitum and housed in plastic cages (temperature 24 ± 1 °C, humidity 55 ± 5 %) with 12 h light dark cycle. All the experiments were conducted in accordance to regulations of Institutional Animal Ethics Committee (IAEC)—NIPER-Hyderabad, India.

Induction of Diabetes and Experimental Design

Diabetes was induced by STZ (55 mg/kg, i.p.) using citrate buffer (pH 4.5). The rats with blood glucose >250 mg/dL after 48 h of diabetes induction were randomly allocated to different groups. A769662 (Chemscene Ltd., NJ, USA) was administered for the last 2 weeks of 8-week-old diabetic rats at 15 and 30 mg/kg, i.p. by dissolving it in saline containing 5 % DMSO. The experimental design and dosage regimen were followed according to the previously established reports of experimental DN [18–20].

Behavioural Parameters

Thermal and Mechanical Hyperalgesia

Thermal hyperalgesia to both hot (45 °C) and cold (10 °C) water was performed. Animals were acclimatised prior to the experiment. The tail flick response latency was observed as endpoint response (cut-off time 15 s) [21]. Mechanical sensitivity to noxious stimuli was assessed using a Vonfrey aesthesiometer and Randall Sellitto callipers (IITC Life Sciences, USA) [22].

Functional Parameters

Motor and Sensory Nerve Conduction Velocities

Motor/sensory nerve conduction velocities (MNCV and SNCV) were calculated using power lab (ADInstruments, Australia). Needle electrodes were used for stimulation of sciatic nerve at sciatic notch or Achilles tendon with 3 V stimulus. The bipolar surface receiving electrodes were kept in foot muscle and the M-wave and H-reflex latencies were measured using Lab chart software. The distance between the stimulation points and latencies were used to determine MNCV/SNCV (m/s) [23].

Sciatic Nerve Blood Flow

Blood flow to the sciatic nerve was measured using laser Doppler oximeter (Moor instruments, UK). Briefly, animals were anaesthetised and their left flank was exposed to visualise the sciatic nerve. Laser probe was placed slightly over the sciatic nerve in an area free from epineurial and perineurial blood vessels. To avoid dehydration of the exposed site, normal saline was applied and the probe was left latent for 10–15 min for stabilisation of the recording. Flux measurements were made for constant time period (10 min) among different animals and reported as arbitrary perfusion units [19].

Biochemical Parameters

Measurement of Glucose Levels

Plasma glucose levels were estimated using GOD-POD kit (Accurex, India) according to the manufacturer's protocol [24].

Measurement of Malondialdehyde

Malondialdehyde (MDA) levels were measured by thiobarbituric acid reactive substance (TBARS) method. Briefly, 0.2 ml of sciatic nerve protein homogenate was mixed with 0.2 ml of 8.1 % SDS, 1.5 ml of 20 % glacial acetic acid solution (pH 3.4) and 1.5 ml of 0.8 % thiobarbituric acid. The resultant mixture was heated on water bath at 95 °C for 60 min. After that, mixture was centrifuged at 10,000 rpm and the absorbance of supernatant was measured at 532 nm. Results are expressed as μM/mg protein [25].

Estimation of Reduced Glutathione

Reduced glutathione (GSH) was measured by Ellman's method in sciatic nerves in accordance to previously established protocol [26]. Sciatic nerve homogenate was centrifuged with 5 % trichloroacetic acid (TCA) to precipitate out the proteins. To the supernatant, 100 μl of Ellman's reagent (dithiobis-2-nitrobenzoic acid (DTNB) in phosphate-buffered saline (PBS) (pH 8)) solution was added and the mixture was then incubated for 10 min at 37 °C and the absorbance was recorded at 412 nm.

Estimation of IL-6 and TNF-α

ELISA estimations were performed using commercial interleukin-6 (IL-6) and tumour necrosis factor alpha (TNF-α) assay kits (eBioscience, USA). The colour developed in the assay plates was read at 450 nm using a spectrophotometer (Spectramax M4).The values obtained were normalised to the protein content and the final values were expressed as pg/mg protein [18].

Estimation of ATP Levels

ATP estimations in sciatic nerves were performed according to kit protocol (Abcam, MA, USA). Briefly, equal volume of the protein supernatant obtained by homogenizing the sciatic nerves was added to an equal volume of mixture of assay buffer, ATP converter, ATP probe, and ATP developer mix. The mixture was incubated in the dark for 30 min and then absorbance reading was taken at 570 nm. The concentration of ATP was represented as nm/mg protein.

DNA Fragmentation and Protein Expression Studies

TUNEL Assay

Terminal deoxynucleotidyl transferase-mediated dUTP nick end labelling (TUNEL) assay was performed to study DNA fragmentation. Sciatic nerves were dehydrated, paraffin embedded, and 4–5-μm sections were made using microtome (Leica). The naked ends of fragmented DNA in the paraffin-embedded nerve sections were labelled with fluorescein isothiocyanate (FITC) using TdT-FragEL kit (Calbiochem, USA). Mounting media containing 4′, 6-diamidino-2-phenylindole (DAPI) was added to sections. TUNEL-positive cells and total number of cells were counted under a fluorescent microscope (Nikon ECLIPSE Ti-U, Japan) [27].

Immunohistochemistry

The nerve sections were deparaffinised and hydrated followed by blocking with bovine serum albumin (BSA) for 15 min. Then, sections were incubated with antibodies for NF-κB P65 subunit and COX-2 (CST) at a dilution of 1:400 at 4 °C overnight followed by incubation with secondary antibody. Thereafter, sections were incubated with a 3, 3-o-diaminobenzidine solution followed by counterstaining with haematoxylin and observed under light microscope [28].

Western Blotting Analysis

Protein samples containing equal protein content across all groups were separated by SDS-PAGE and transferred to PVDF membrane. After blocking with 3 % BSA, membranes were incubated with antibodies P-AMPK, AMPK, NRF-1, Beclin1, LC3 A/B, NF-κB, COX-2, β-actin (Cell Signalling Technology, USA) (1:1000), and PGC-1α, SIRT1, iNOS, Tfam (Santa cruz, USA) (1:1000) for 12 h at 4 °C. After washing, membranes were incubated with HRP-conjugated secondary antibodies (Cell Signalling Technology, USA) (1:20000). Chemiluminescence was visualised using a Fusion-FX chemiluminescence imager (Vilber Lourmat, Germany). The relative band densities were quantified by densitometry using ImageJ software (version 1.48, NIH, USA) [27].

Neuronal Cell Culture

The neuro2a (N2A) cell line from National Centre for Cell Sciences (NCCS, Pune, India) were grown in minimum essential medium (MEM) (containing 5 mM glucose) supplemented with 10 % fetal bovine serum (FBS), glutamine (2 mM), streptomycin/penicillin (1 %), at 37 °C, in a humidified atmosphere of 95 % air and 5 % CO_2. High glucose condition was created by adding 25 mM glucose to medium (final concentration in medium 30 mM).

Assessment of Neurite Outgrowth

N2A cells were plated in a 12-well plate at a density of 5000 cells/well. After 12 h, cells were treated with glucose and A769662. Five random fields (100–200 cells/well) were examined using a phase contrast microscope (Nikon ECLIPSE

Table 1 Effect of 2-week treatment with A769662 (15 and 30 mg/kg) on various behavioural, biochemical and functional characteristics of DN

Parameter	ND	STZ-D	STZ-D + A-15	STZ-D + A-30
MNCV (m/s)	60.26 ± 1.62	39.70 ± 0.91^^	44.75 ± 4.53	51.40 ± 3.20*
SNCV (m/s)	55.58 ± 1.54	34.00 ± 1.81^^^	43.03 ± 6.34	49.92 ± 2.80**
NBF (PU)	102.55 ± 1.83	46.43 ± 2.37^^^	55.76 ± 2.63	89.30 ± 5.18***
Tail withdrawal latency to hot stimuli (s)	13.62 ± 0.44	4.74 ± 0.11^^^	7.45 ± 1.09	11.89 ± 1.43***
Tail withdrawal latency to cold stimuli (s)	14.22 ± 0.28	5.03 ± 0.36^^^	8.80 ± 0.87**	13.97 ± 0.97***
Paw withdrawal threshold (g)	63.68 ± 1.18	44.70 ± 1.14^^^	53.32 ± 1.34*	61.30 ± 2.29***
Paw withdrawal pressure (g)	198.30 ± 4.91	100.17 ± 1.73^^^	145.15 ± 8.35***	186.47 ± 5.11***
Plasma glucose (mg/dl)	95.91 ± 9.47	403.80 ± 18.22^^^	361.68 ± 19.44	385.31 ± 33.44
Average body weight (gm)	326.67 ± 7.27	210.00 ± 4.62^^^	223.67 ± 6.65	226.67 ± 3.53
MDA (μM/mg)	5.44 ± 1.04	30.91 ± 1.95^^^	22.79 ± 0.70*	10.19 ± 1.03***
GSH (μM/mg)	34.93 ± 0.94	18.15 ± 0.63^^^	21.60 ± 0.53	25.50 ± 0.51**

Results are expressed as mean ± SEM ($n = 6$)

ND non-diabetic, *STZ-D* diabetic, *STZ-D + A-15* diabetic rats treated with A769662 at 15, *STZ-D + A-30* diabetic rats treated with A769662 at 30 mg/kg

^^$p < 0.01$, ^^^$p < 0.001$ vs ND, *$p < 0.05$, **$p < 0.01$, ***$p < 0.001$ vs STZ-D

Ti-U, Japan). Neurite length was measured in at least 30 cells per randomly chosen fields by using ImageJ (Version 1.48, NIH, USA) software. The number of neurite outgrowths, defined as axon-like extensions that were double or more than the diameter of cell body was recorded. The percentage neurite bearing cells (%) is the number of neurite bearing cells divided by the total number of cells and then multiplied by 100 [29].

Measurement of Intracellular ROS by DCFDA Staining

Cells were seeded in 6-well plate at a density of 5×10^4 cells/cm^2. After 24-h incubation, they were exposed to drug solutions with indicated concentrations for 6 h. Then, cells were loaded with 5 μM H2DCF-DA for 20 min and fluorescence was visualised using a fluorescence microscope (Nikon ECLIPSE Ti-U, Japan) [30].

Assessment of Mitochondrial Superoxide Anion (O_2^-) by MitoSOX staining

N2A cells were plated in a 6-well plate at a density of 50,000 cells/well and incubated overnight. After 24 h, cells were subjected to treatment for 6 h. The cells were then incubated with 5 μM MitoSOX for 10 min at 37 °C, protected from light, washed and processed for imaging under a fluorescent microscope [31].

Assessment of Mitochondrial Membrane Potential ($\Delta\psi_m$) by JC-1 Staining

N2A cells were seeded in 6-well plate at a density of 5×10^4 cells/cm^2 and after 24-h incubation exposed to drug solutions with indicated concentrations for 6 h. JC-1 (5 μM/ml) was prepared in phosphate buffered saline (PBS) and cells were incubated for 20 min with JC-1. Then, cells were visualised under fluorescent microscope [32].

Statistical Analysis

The results were expressed as mean ± SEM. Statistical comparisons were made with "Bonferroni's multiple comparison test". The intergroup variations were measured by one-way analysis of variance using the GraphPad Prism (version 5.0., USA). Results with $p < 0.05$ were considered to be statistically significant.

Results

Glucose levels in the diabetic rats were significantly elevated ($p < 0.001$). Significant ($p < 0.001$) loss in body weights were observed in diabetic rats when compared to normal rats (Table 1). Two-week treatment with A769662 (15 and 30 mg/kg, i.p) showed no significant effect on plasma glucose and body weight changes in treated animals.

AMPK Activation by A769662 Normalises the Nerve Functional Changes and Reduces Pain Associated With DN

Sensorimotor responses to thermal and mechanical stimuli ($p < 0.001$) were significantly decreased in diabetic rats (Table 1). A769662 treatment for 2 weeks significantly attenuated the pain hypersensitivity and resulted in improved tail flick latencies and paw withdrawal thresholds ($p < 0.001$ at

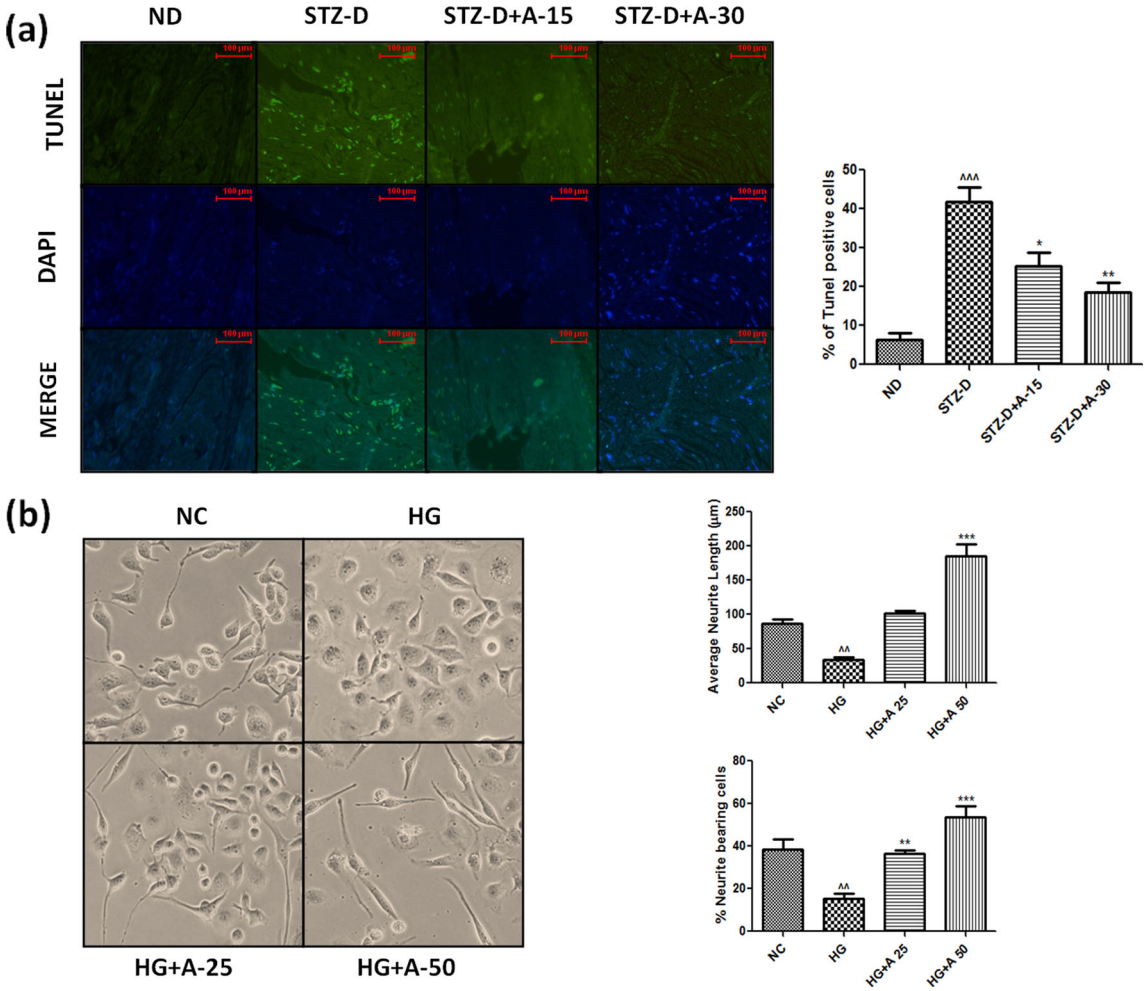

Fig. 1 Effect of A769662 administration on oxidative DNA damage in STZ-induced rats and neuritogenesis in high glucose-exposed N2A cells: **a** fluorescent microscopic images of TUNEL-positive cells and corresponding DAPI-stained sciatic nerve microsection and graphical representations of average (%) TUNEL-positive cells. **b** Representative bright field microscopic images of N2A cells captured after 12 h exposure to glucose (30 mM) and A769662 (25 and 50 μM) (×20) and graphical representation of average neurite length (μM) and percentage neurite bearing cells. Values are expressed as mean ± SEM ($n = 3$). *ND*: non-diabetic, *STZ-D*: diabetic, *STZ-D + A-15* are *STZ-D + A-30* are diabetic rats treated with A769662 at 15 and 30 mg/kg respectively. ^^$p < 0.01$ vs ND, *$p < 0.05$ vs STZ-D. *NC*: normal N2A cells, *HG*: high glucose (30 mM)-exposed N2A cells, *HG + A 25* and *HG + A 50* are high glucose-insulted cells coincubated with A769662 at 25 and 50 μM, respectively. ^^$p < 0.01$ vs NC, **$p < 0.01$, ***$p < 0.001$ vs HG

30 mg/kg dose) in treated diabetic animals. Marked reduction in the MNCV ($p < 0.01$) and SNCV ($p < 0.001$) was observed in diabetic rats when compared to normal rats (Fig. 1). NBF was also significantly ($p < 0.001$) impaired in diabetic rats when compared to normal rats. Treatment with A769662 to the diabetic rats significantly restored these functional deficits associated with diabetes (Table 1).

AMPK Activation Reverses Oxidative Stress-Associated Changes in High Glucose-Exposed N2A Cells and STZ-Induced Rats

An increased DCF fluorescence in high glucose conditions after 6 h of exposure indicates the glucose-driven ROS generation. Coincubation of high glucose-treated cells with A769662 at 25 and 50 μM significantly attenuated ROS generation in a dose-dependent manner (Fig. 3). An elevated number of TUNEL-positive cells ($p < 0.01$) in the nerve microsections of diabetic rats were observed (Fig. 1a). Significant increase in MDA ($p < 0.001$) and diminished GSH ($p < 0.001$) level in the sciatic nerves of diabetic rats were also observed (Table 1). A769662 treatment significantly reduced TUNEL-positive cells ($p < 0.05$) (Fig. 1a), inhibited the lipid peroxidation ($p < 0.05$ at 15 mg/kg and $p < 0.001$ at 30 mg/kg) and improved the antioxidant defence by improving glutathione levels ($p < 0.01$ at 30 mg/kg) in the sciatic nerves of treated diabetic rats.

AMPK Activation Promotes Neuritogenesis in High Glucose-Insulted N2A Cells

Exposure to 30 mM glucose reduced average neurite length ($p < 0.01$) and neurite generation when compared to the

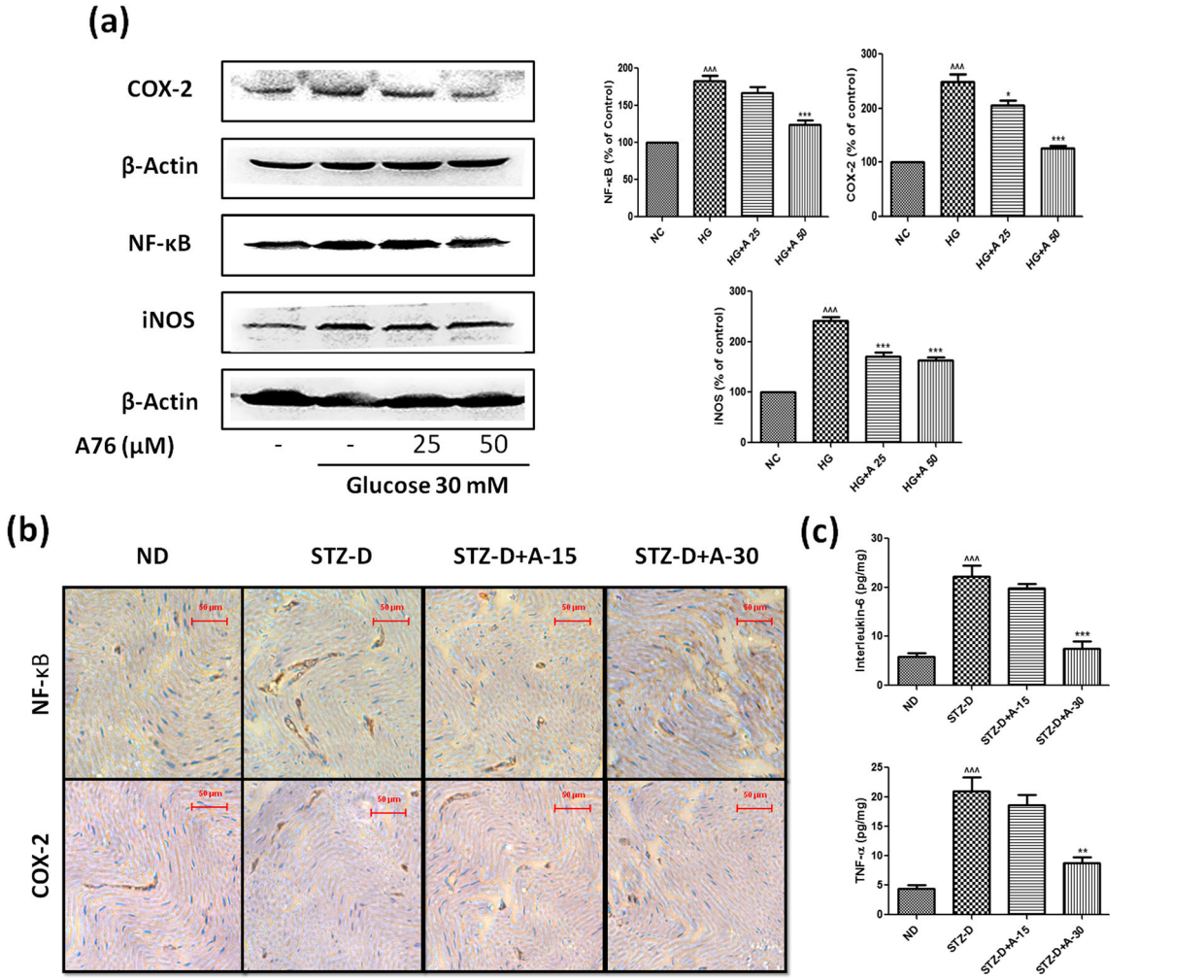

Fig. 2 Effect of A769662 on high glucose-induced inflammatory changes in N2A cells and inflammatory marker expression in sciatic nerves of STZ-induced rats. **a** Representative immunoblot images of iNOS, COX-2, NF-κB, β-actin and corresponding graphical representations of densitometric analysis. **b** Pictorial representations of immunoperoxidase-stained nerve sections for NF-κB (*first row*) and COX-2 (*second row*). *Bar graphs* (**c**) represent the levels of IL-6 and TNF-α in sciatic nerve lysates. Results are expressed as mean ± SEM ($n = 3$). *NC*: normal N2A cells, *HG*: high glucose (30 mM)-exposed N2A cells, *HG + A 25* and *HG + A 50* are high glucose-insulted cells coincubated with A769662 at 25 and 50 μM, respectively. ^^^$p < 0.001$ vs NC, *$p < 0.05$, ***$p < 0.001$ vs HG. *ND*: non-diabetic, *STZ-D*: diabetic, *STZ-D + A-15* and *STZ-D + A-30* are diabetic rats treated with A769662 at 15 and 30 mg/kg, respectively. ^^^$p < 0.001$ vs ND, **$p < 0.01$ and ***$p < 0.001$ vs STZ-D

normal N2A cells (Fig. 1b). Average neurite length and average neurite-bearing cells have been considerably increased with A769662 treatment in a dose-dependent manner even under high glucose conditions (Fig. 1b).

A769662 Treatment Ameliorates Neuroinflammation in High Glucose-Exposed N2A Cells and Peripheral Nerves of STZ-Induced Rats

High glucose exposure to N2A cells caused significant increase in NF-κB level ($p < 0.001$) and inflated proinflammatory COX-2 and iNOS proteins ($p < 0.001$) when compared with the normal N2A cells (Fig. 2a). A769662 treatment for 24 h to high glucose-insulted N2A cells decreased NF-κB levels. Reduction in p65, COX-2 and iNOS protein expression resulted after A769662 administration (Fig. 2a). Chronic diabetes significantly elevated the NF-κB-mediated neuroinflammation as evident by enhanced levels of IL-6 ($p < 0.001$) and TNF-α ($p < 0.001$) in the sciatic nerve lysates (Fig. 2c) and increased immunopositivity towards p65 ($p < 0.001$) and COX-2 ($p < 0.001$) in the nerve microsections of diabetic rats (Fig. 2b). A769662 treatment significantly reduced the expression of IL-6 ($p < 0.001$) and TNF-α ($p < 0.01$) and reduced the expression of NF-κB ($p < 0.01$) and COX-2 ($p < 0.05$) when compared to STZ-induced rats (Fig. 2b).

High Glucose-Mediated Mitochondrial Dysfunction in N2A Cells and Reversal by AMPK Activation

High glucose (30 mM) exposure led to increased generation of mitochondrial specific superoxide as evident by elevated MitoSOX fluorescence and mitochondrial membrane

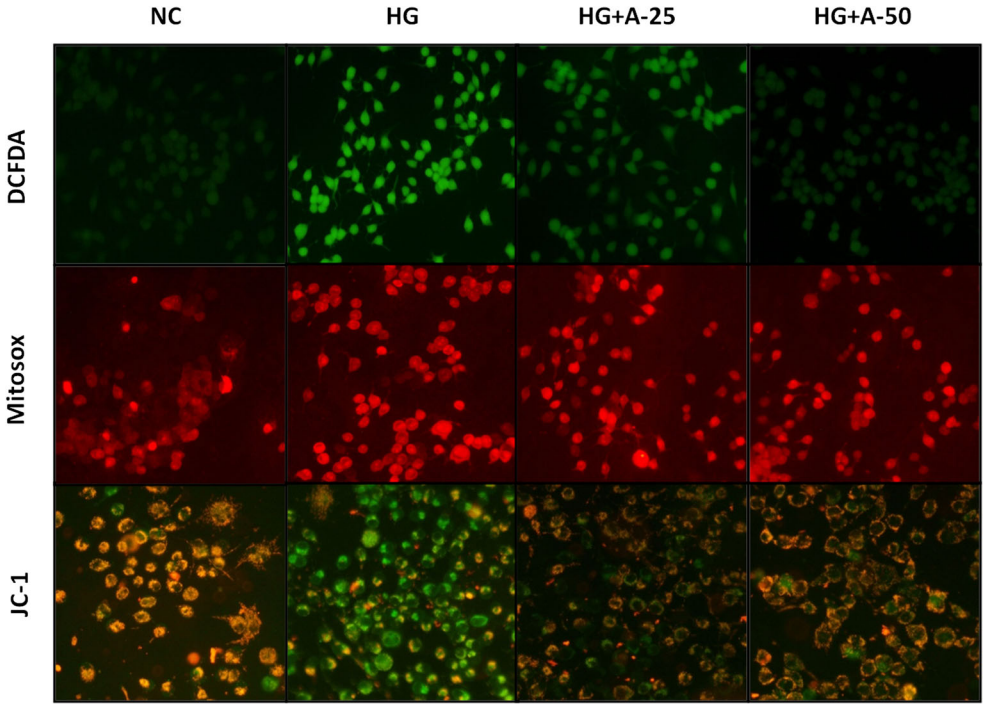

Fig. 3 Effect of high glucose exposure and AMPK activation on intracellular ROS levels, mitochondrial superoxide generation and mitochondrial membrane potential: representative DCF fluorescent images of ROS generation (*first panel*) in N2A cells exposed to high glucose and A769662. MitoSOX staining for the determination of mitochondrial superoxide generation (*second panel*) in N2A cells. JC-1 stained N2A cells for the determination of mitochondrial membrane potential. *Orange fluorescence* indicates the aggregated form of JC-1 and *green colour* is that of monomeric form. *NC*: normal N2A cells, *HG*: high glucose (30 mM)-exposed N2A cells, *HG + A 25* and *HG + A 50* are high glucose-insulted cells coincubated with A769662 at 25 and 50 μM, respectively

depolarisation as confirmed by increased JC-1 monomer green florescence in N2A cells (Fig. 3). Treatment with A769662 to the high glucose-exposed cells reduced the mitochondria generation of superoxide and ensured repolarisation of mitochondrial membrane (red fluorescence) (Fig. 3).

A769662 Treatment Increases AMPK Phosphorylation and Augments Mitochondrial Biogenesis and Autophagy in High Glucose-Treated N2A cells

High glucose exposure caused significant ($p < 0.001$) impairment in AMPK phosphorylation and its activity (Fig. 4). A769662 treatment enhanced Thr 172 phosphorylation of AMPK in high glucose-insulted cells in a dose-dependent manner ($p < 0.001$ at 25 and 50 μM). Significant reductions ($p < 0.001$) in the levels of SIRT1 and PGC-1α, NRF1 and Tfam signalling were also observed in high glucose-exposed cells (Fig. 4). High glucose exposure impaired the formation of autophagosomes, as evident from reduced levels of Beclin1 ($p < 0.01$) and LC3-II ($p < 0.001$) proteins when compared with their basal expression (Fig. 4). A769662 exposure resulted in increase in expression of PGC1α ($p < 0.001$ at 50 μm), NRF1 ($p < 0.01$ at 50 μm), SIRT1 ($p < 0.001$) at higher dose (50 μm) and Tfam ($p < 0.05$ and $p < 0.001$ at 25 and 50 μm respectively), Beclin1 ($p < 0.01$ at 50 μm) and LC3-II ($p < 0.001$ at both doses of A7696622) in a dose-dependent manner.

Diabetes Compromises Mitochondrial Biogenesis, Turnover and Functional Capacity in the Sciatic Nerves of STZ-Induced Diabetic Rats and A769662 Administration Corrected These Anomalies

A profound reduction in Thr 172 phosphorylation of AMPK ($p < 0.001$) in the diabetic rats was observed when compared to the normal healthy rats (Fig. 5a). Further, PGC-1α ($p < 0.001$) and NRF-1 ($p < 0.001$) expression in the STZ-induced rats were reduced when compared with the normal rats. Chronic diabetes in rats reduced Beclin1 levels ($p < 0.001$) in the sciatic nerves (Fig. 5a). A769662 treatment for 2 weeks reversed AMPK inactivation and associated mitochondrial biogenesis and autophagy deficits in diabetic rats. ATP content was diminished in sciatic nerves of diabetic rats (STZ-D 0.65 ± 0.13 nM vs ND 1.98 ± 0.09 nM), and A769662 significantly ($p < 0.001$) elevated mitochondrial ATP production in treated rats (Fig. 5b).

Discussion

The results obtained in this study indicated possible involvement of AMPK signalling in diabetic neuropathy and associated mitochondrial dysfunction. AMPK activation efficiently counteracted the diabetes-induced thermal and mechanical hyperalgesia as well conduction and nerve blood flow deficits.

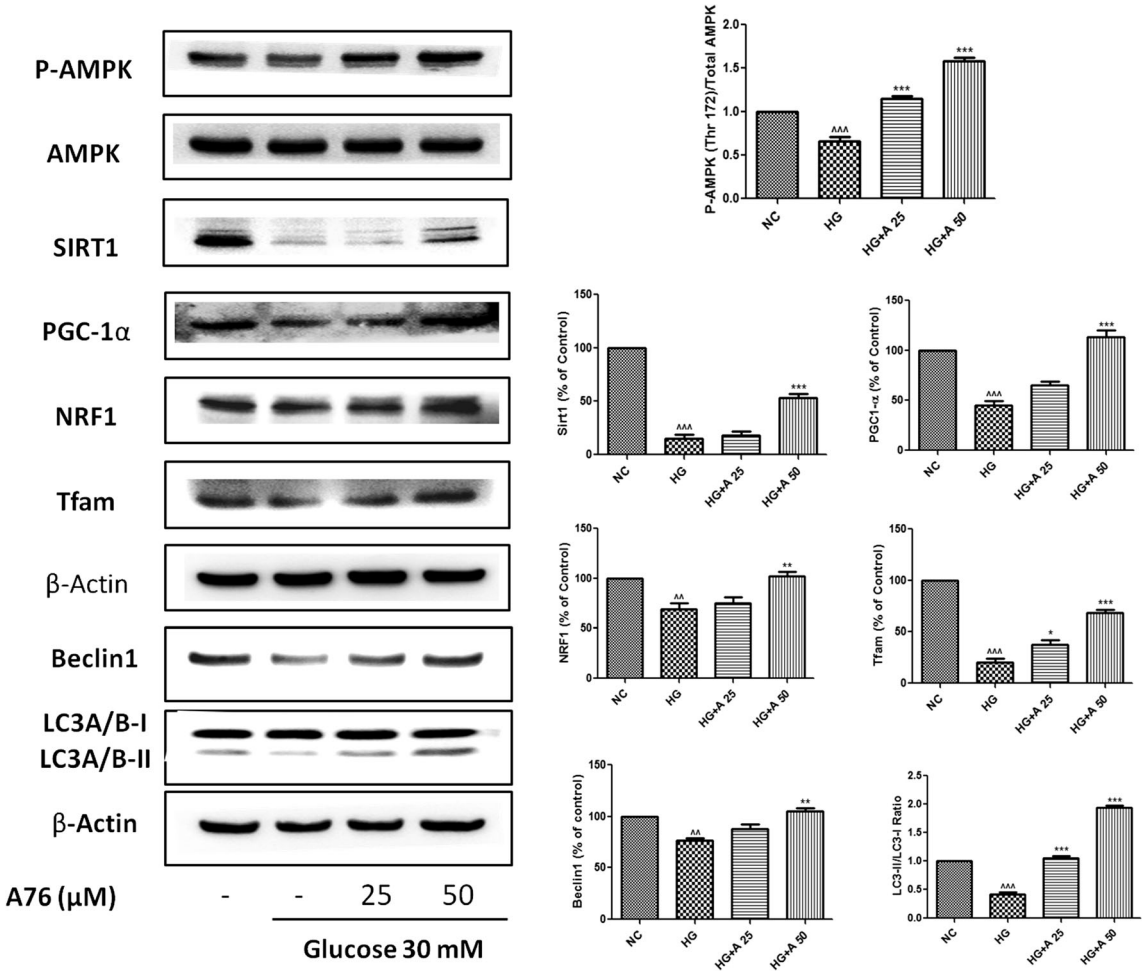

Fig. 4 Effect of A769662 treatment on protein expression changes in high glucose-insulted N2A cells: immunoblot images of p-AMPK, total AMPK, SIRT1, PGC-1α, NRF-1, Tfam, LC3-II, Beclin1 and β-actin. *Bar graphs* represent densitometric analysis of respective western blots. Results are expressed as mean ± SEM ($n = 3$). *NC*: normal N2A cells, *HG*: high glucose (30 mM)-exposed N2A cells, *HG + A 25* and *HG + A 50* are high glucose-insulted cells coincubated with A769662 at 25 and 50 μM, respectively. ^^$p < 0.01$, ^^^$p < 0.001$ vs NC, *$p < 0.05$, **$p < 0.01$, ***$p < 0.001$ vs HG

Reduced Thr 172 phosphorylation of AMPK resulted in compromised mitochondrial biogenesis and autophagosome formation in diabetic rats. This study also supported the fact that activation of AMPK enhances PGC-1α-mediated mitochondrial biogenesis and inhibits the pathological activation of NF-κB-induced neuroinflammation under hyperglycaemic conditions.

Neurons require copious amount of energy (ATP) to meet their high energetic demands such as maintenance of large electrochemical gradients across the cell membrane and dendritic arborisation for neurotransmission [33]. Impaired neuronal sprouting under hyperglycaemic conditions is identified as outcome of reduced insulinotropic or neurotrophic support to the nerves [34]. The increase in the neurite length and neurite-bearing capacity by AMPK activation confirmed the critical importance of ATP requirement in the formation of growth cone and sprouting of neurites [35, 36].

Reduced nerve conduction velocities in diabetic rats leads to impaired and altered sensory signalling in the peripheral limbs which manifests in the form of hyperalgesia and allodynia, the hallmark symptoms of neuropathic pain [37]. AMPK activation was reported for its protective effect against allodynia and hyper excitability in trauma-induced neuropathic pain [17]. Improvement in the conduction deficits and reduced pain hypersensitivity in diabetic animals by A769662 administration indicates that the AMPK modulation might have exerted neuroprotection via limiting inflammatory damage to myelin layer of peripheral nerves and reduced nociceptive sensitisation by inflammatory mediators [38]. NF-κB-mediated neuroinflammation is also known to exert its effect on vascular deficits seen in DN via induction of COX-2 and iNOS. COX-2 has previously been identified to alter Na^+-K^+ activity in the nerves and enhances the production of vasoconstrictor thromboxane [39]. iNOS production is also known to produce aberrant NO generation and can result in nitrosative damage [40]. A769662 administration enhanced the peripheral blood supply to the neurons in diabetic animals at both the doses which may be due to inhibition of NF-κB activation or eNOS activation by AMPK [41].

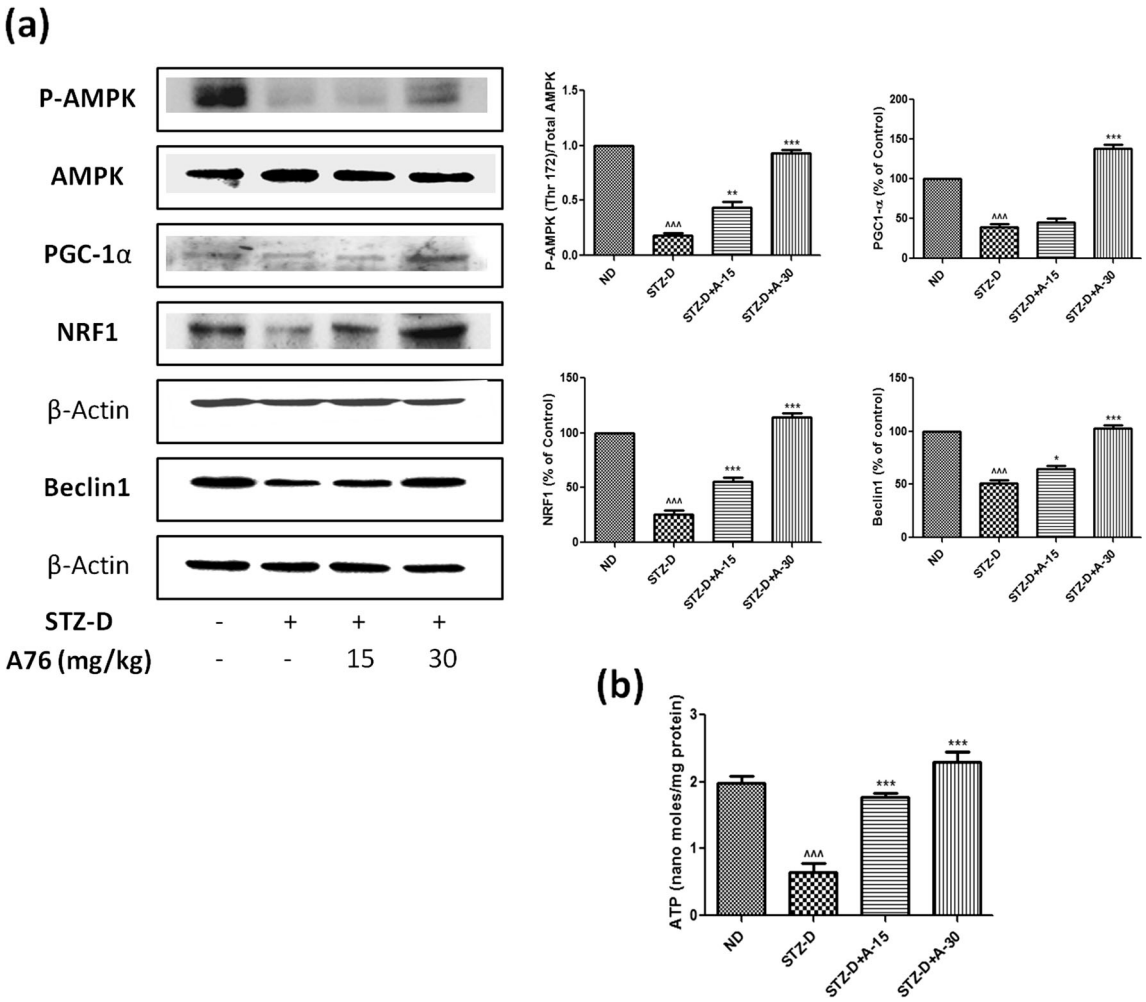

Fig. 5 Effect of 2-week administration of A769662 on protein expression changes and ATP levels in STZ-induced rats: **a** western blot images indicating the expression of p-AMPK, total AMPK, PGC-1α, NRF-1, Beclin1 and β-actin protein in sciatic nerve lysates of normal and STZ-induced rats. *Graphical representations* indicate densitometric analysis for respective western blots. Average ATP levels (**b**) measured in sciatic nerve lysates of normal and STZ-induced rats. Results are expressed as mean ± SEM ($n = 3$). *ND*: non-diabetic, *STZ-D*: diabetic, *STZ-D + A-15* and *STZ-D + A-30* are diabetic rats treated with A769662 at 15 and 30 mg/kg, respectively. ^^^$p < 0.001$ vs ND, *$p < 0.05$,**$p < 0.01$, ***$p < 0.001$ vs STZ-D

Hyperglycaemia-mediated ROS generation and subsequent activation of inhibitory kappa kinase (IKK) result in aberrant activation of NF-κB signalling [42]. Hyperglycaemia-induced neuroinflammation was evident through increased immunoperoxidase staining for NF-κB, COX-2 in the sciatic nerves of diabetic rats and elevated levels of NF-κB, COX-2 and iNOS in high glucose-exposed N2A cells. AMPK activation by A769662 reduced the neuroinflammatory manifestations associated with NF-κB signalling in both STZ-induced rats as well as hyperglycaemia-exposed N2A cells which is in line with earlier reports on AMPK-directed NF-κB inhibition [43]. Oxidative stress-associated damage was evident from increased lipid peroxidation and reduced glutathione content observed in STZ-induced rats and ROS-mediated DNA fragmentation in sciatic nerve microsections which concurred earlier observations in experimental DN [44, 45]. AMPK activation reduced the overall ROS generation under hyperglycaemia and thus prevented oxidative damage in sciatic nerves of diabetic rats. These features were anticipated to be observed due to improvement in mitochondrial performance by AMPK activation [46].

Unlike most tissues in the body, glucose entry into the neuronal cells does not depend on the insulin but is diffusion-mediated and thus makes the neurons susceptible to hyperglycaemic load [47]. High glucose entered in the cell is directed to the mitochondrial electron transport chain (ETC) through primary metabolic pathways such as glycolysis and tricarboxylic acid (TCA) cycle. Increased shuttling of the energy equivalents through ETC chain can result in leakage of electrons and generation of superoxide. The generated superoxide may damage mitochondrial DNA, which results in error-prone transcription and translation of defective mitochondrial components [46]. In the present study, hyperglycaemia-induced increase in the mitochondrial superoxide production and corresponding depolarisation of inner mitochondrial membrane clearly indicated the glucose-driven

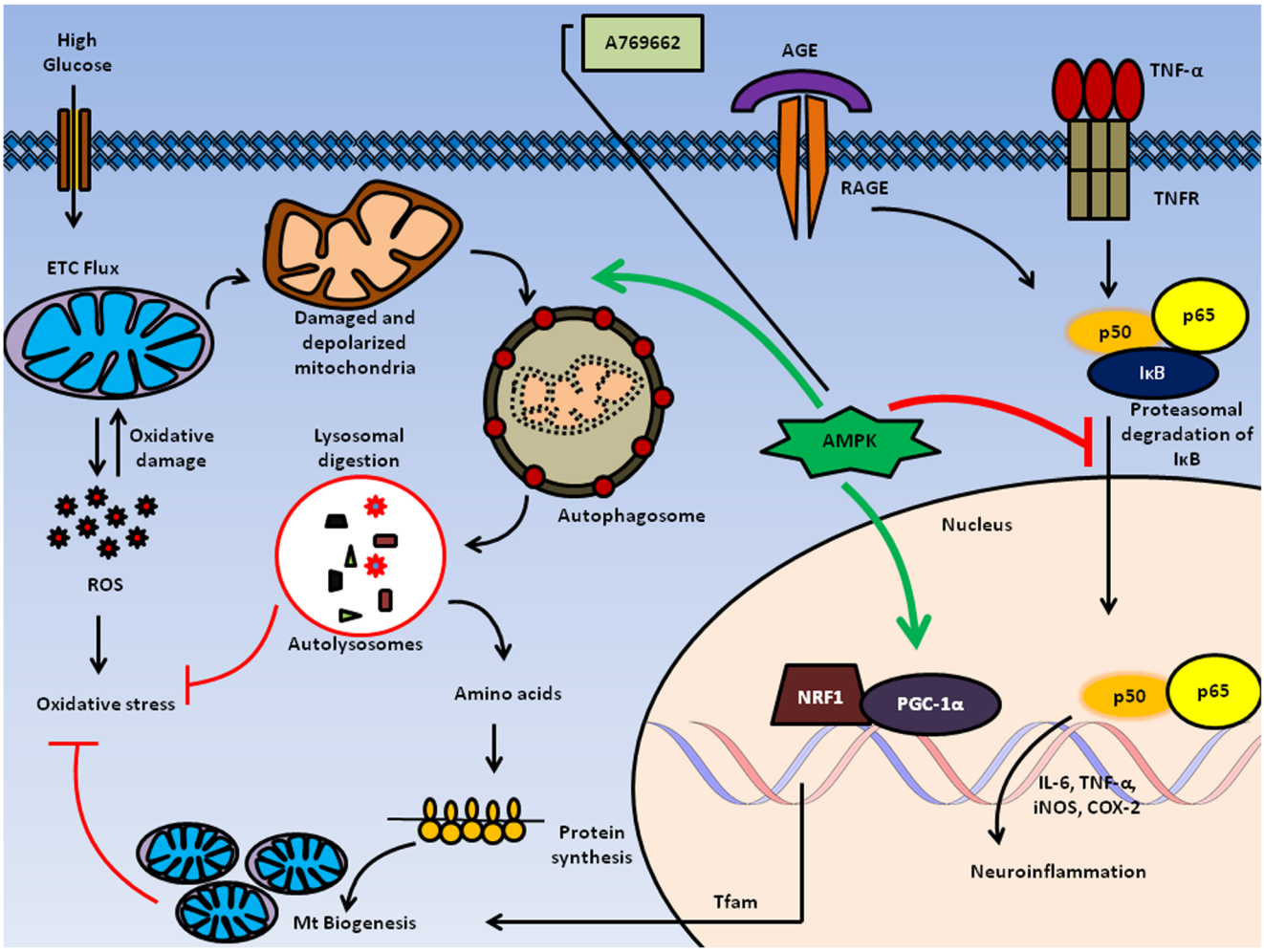

Fig. 6 Probable mechanism of AMPK-mediated neuroprotection in experimental DN: high glucose-driven ETC flux in mitochondria results in ROS generation, which can damage the mitochondrial components. Oxidative damage to mitochondria makes them labelled for recycling through mitophagy. Autophagosome encloses the damaged mitochondria which eventually fuse with lysosomes to degrade the mitochondria and release the raw materials into cytoplasm. The released components such as amino acids can be used for protein synthesis. Glucose-induced AGE and its further association with RAGE are also involved in nuclear localisation of NF-κB heterodimer and thus enhance proinflammatory mediators such as IL-6, TNF-α, COX-2 release which results in neuroinflammation. TNF-α can further positively modulate this NF-κB signalling through TNFR facilitation. AMPK activation by A769662 can induce the autophagy through facilitation of autophagosome formation (Ulk1 activation). AMPK can also inhibit the NF-κB signalling and thus halts the NF-κB-induced neuroinflammation. AMPK-mediated phosphorylation of PGC-1α facilitates NRF1 transcription and mitochondrial biogenesis. The newly synthesised healthy mitochondria and removal of damaged mitochondria by autophagy have an overall impact of reducing the ROS-mediated oxidative stress inside the cellular system. (*AGE*: advanced glycation end products, *AMPK*: adenosine monophosphate kinase, *COX-2*: cycloxygenase2, *ETC*: electron transport chain, *IL-6*: interleukin6, *NF-κB* : nuclear factor kappa light chain enhancer of B cells, *NRF1*: nuclear respiratory factor1, *PGC-1α*: peroxisome proliferator-activated receptor gamma coactivator 1 alpha, *RAGE*: receptor for AGE, *ROS*: reactive oxygen species, *TNF-α*: tumour necrosis factor alfa, *Tfam*: transcription factor A, mitochondrial, *TNFR*: tumour necrosis factor receptor, *Ulk1*: unc-51-like autophagy-activating kinase 1)

mitochondrial dysfunction. Restoration of mitochondrial membrane potential by A769662 exposure supports the observation of reduced superoxide generation and maintenance of electrochemical gradient across the inner membrane.

Recent studies have evaluated the role of healthy mitochondrial biogenesis and its therapeutic benefit in the neurodegenerative disorders [48–50]. Indeed, mitochondrial transcription factor A (Tfam) overexpressed rats were protected from nerve conduction deficits and mitochondrial degeneration observed in experimental DN [51]. In our study, we also observed hyperglycaemia-directed reduction of PGC-1α, the master regulator of mitochondrial biogenesis. The reduced expression of PGC-1α, NRF1 and Tfam under hyperglycaemic condition further fortifies our observation of reduced mitochondrial biogenesis as contributor to the pathophysiology of DN. Treatment with A769662 results in increased Thr 172 phosphorylation of AMPK in both STZ-induced rats as well as 30-mM-exposed N2A cells. Further AMPK activation resulted in enhanced mitochondrial biogenesis under diabetic condition as evident by increased expression of PGC-1α, NRF1 and Tfam. AMPK

activation also facilitated SIRT1 signalling in the neurons, which may be due to overall adjustment of cellular NAD energy pool. The critical observation was the measurement of ATP levels in the sciatic nerves of STZ-induced rats, where reduced ATP generation under diabetic condition indicate the degree of mitochondrial functional impairment due to ETC dysfunction. AMPK activation by A769662 enhanced the ATP production under hyperglycaemic conditions, which may point towards replenishing the metabolic balance via increased production of cellular energy.

Autophagy is a neuroprotective measure to reduce the accumulation of damaged cellular components and protein aggregates in neurological disorders [52]. We found reduced formation of autophagosomes under hyperglycaemic conditions, as evident from the reduced expression of LC3B-II and Beclin1. Beclin1 with the help of class III PI3K enzyme, Vsp34, helps in formation of phagophore and recruitment of other autophagy-related proteins such as LC3B-II to the phagophore which leads to formation of autophagosomes [53]. A769662 treatment resulted in enhanced cleavage of LC3B-II from LC3B-I and enhanced expression of Beclin1, an indication for the induction of autophagy. This elevated autophagosome formation results in clearance of damaged or degenerated mitochondria which further improved mitochondrial function by A769662 [54].

Diabetic condition creates a maladaptive inhibition of AMPK signalling by mimicking a nutrient excess condition inside neurons. However, excess glucose is underutilised for producing ATP; instead, it enhances the accumulation of depolarised, damaged mitochondria inside the cells. Thus, the high glucose-mediated mitochondrial dysfunction results in a futile mitochondrial performance i.e. reduced ATP generation and increased ROS production. AMPK activation facilitated the clearance of damaged mitochondria and also enhances the biogenesis of healthy mitochondria, thus helps to maintain a healthy mitochondrial phenotype under the conditions of experimental DN (Fig. 6). The study serves as a substantial evidence of harnessing the therapeutic benefit afforded by AMPK activation and paves the way for further exploration of therapeutic molecules targeting AMPK in diabetes-associated microvascular complications.

Acknowledgments The authors would like to acknowledge the financial support provided by the Department of Pharmaceuticals, Ministry of Chemicals and Fertilizers, Government of India for carrying out this work.

Compliance with Ethical Standards

Conflict of Interest The authors declare that they have no conflicts of interest.

References

1. Forbes JM, Cooper ME (2013) Mechanisms of diabetic complications. Physiol Rev 93(1):137–188
2. Negi G, Kumar A, Joshi RP, Sharma SS (2011) Oxidative stress and Nrf2 in the pathophysiology of diabetic neuropathy: old perspective with a new angle. Biochem Biophys Res Commun 408(1):1–5
3. Vinik AI, Mehrabyan A (2004) Diabetic neuropathies. Med Clin N Am 88(4):947–999
4. Schmeichel AM, Schmelzer JD, Low PA (2003) Oxidative injury and apoptosis of dorsal root ganglion neurons in chronic experimental diabetic neuropathy. Diabetes 52(1):165–171
5. Vincent AM, Brownlee M, Russell JW (2002) Oxidative stress and programmed cell death in diabetic neuropathy. Ann N Y Acad Sci 959(1):368–383
6. Cameron NE, Cotter MA (2008) Pro-inflammatory mechanisms in diabetic neuropathy: focus on the nuclear factor kappa B pathway. Curr Drug Targets 9(1):60–67
7. Ziegler D (2008) Treatment of diabetic neuropathy and neuropathic pain. Diabetes Care 31(Suppl 2):S255–221
8. Jensen TS, Backonja M-M, Jiménez SH, Tesfaye S, Valensi P, Ziegler D (2006) New perspectives on the management of diabetic peripheral neuropathic pain. Diabetes Vasc Dis Res 3(2):108–119
9. Kann O, Kovács R (2007) Mitochondria and neuronal activity. Am J Physiol-Cell Physiol 292(2):C641–C657
10. Kukidome D, Nishikawa T, Sonoda K, Imoto K, Fujisawa K, Yano M, Motoshima H, Taguchi T et al (2006) Activation of AMP-activated protein kinase reduces hyperglycemia-induced mitochondrial reactive oxygen species production and promotes mitochondrial biogenesis in human umbilical vein endothelial cells. Diabetes 55(1):120–127
11. Mihaylova MM, Shaw RJ (2011) The AMPK signalling pathway coordinates cell growth, autophagy and metabolism. Nat Cell Biol 13(9):1016–1023
12. Austin S, St-Pierre J (2012) PGC1α and mitochondrial metabolism–emerging concepts and relevance in ageing and neurodegenerative disorders. J Cell Sci 125(21):4963–4971
13. Palikaras K, Tavernarakis N (2014) Mitochondrial homeostasis: the interplay between mitophagy and mitochondrial biogenesis. Exp Gerontol 56:182–188
14. Chowdhury SKR, Smith DR, Saleh A, Schapansky J, Marquez A, Gomes S, Akude E, Morrow D et al (2012) Impaired adenosine monophosphate-activated protein kinase signalling in dorsal root ganglia neurons is linked to mitochondrial dysfunction and peripheral neuropathy in diabetes. Brain 135(6):1751–1766
15. Choi J, Chandrasekaran K, Inoue T, Muragundla A, Russell JW (2014) PGC-1α regulation of mitochondrial degeneration in experimental diabetic neuropathy. Neurobiol Dis 64:118–130
16. Göransson O, McBride A, Hawley SA, Ross FA, Shpiro N, Foretz M, Viollet B, Hardie DG et al (2007) Mechanism of action of A-769662, a valuable tool for activation of AMP-activated protein kinase. J Biol Chem 282(45):32549–32560
17. Melemedjian OK, Asiedu MN, Tillu DV, Sanoja R, Yan J, Lark A, Khoutorsky A, Johnson J et al (2011) Targeting adenosine monophosphate-activated protein kinase (AMPK) in preclinical models reveals a potential mechanism for the treatment of neuropathic pain. Mol Pain 7(1):70
18. Kumar A, Sharma SS (2010) NF-kappaB inhibitory action of resveratrol: a probable mechanism of neuroprotection in experimental diabetic neuropathy. Biochem Biophys Res Commun 394(2):360–365
19. Kumar A, Negi G, Sharma SS (2012) Suppression of NF-κB and NF-κB regulated oxidative stress and neuroinflammation by BAY 11–7082 (IκB phosphorylation inhibitor) in experimental diabetic neuropathy. Biochimie 94(5):1158–1165
20. Negi G, Sharma SS (2015) Inhibition of IκB kinase (IKK) protects against peripheral nerve dysfunction of experimental diabetes. Mol Neurobiol 51(2):591–598

21. Narenjkar J, Roghani M, Alambeygi H, Sedaghati F (2011) The effect of the flavonoid quercetin on pain sensation in diabetic rats. Basic Clin Neurosci 2(3):51–57
22. Sandireddy R, Yerra VG, Komirishetti P, Areti A, Kumar A (2015) Fisetin imparts neuroprotection in experimental diabetic neuropathy by modulating Nrf2 and NF-κB pathways Cell Mol Neurobiol:1–10. doi:10.1007/s10571-015-0272-9
23. Ali S, Driscoll HE, Newton VL, Gardiner NJ (2014) Matrix metalloproteinase-2 is downregulated in sciatic nerve by streptozotocin induced diabetes and/or treatment with minocycline: Implications for nerve regeneration. Exp Neurol 261:654–665
24. Kumar A, Kaundal RK, Iyer S, Sharma SS (2007) Effects of resveratrol on nerve functions, oxidative stress and DNA fragmentation in experimental diabetic neuropathy. Life Sci 80(13):1236–1244
25. Ohkawa H, Ohishi N, Yagi K (1979) Assay for lipid peroxides in animal tissues by thiobarbituric acid reaction. Anal Biochem 95(2):351–358
26. Moron MS, Depierre JW, Mannervik B (1979) Levels of glutathione, glutathione reductase and glutathione S-transferase activities in rat lung and liver. Biochim Biophys Acta-Gen Subj 582(1):67–78
27. Negi G, Kumar A, Sharma SS (2011) Melatonin modulates neuroinflammation and oxidative stress in experimental diabetic neuropathy: effects on NF-kB and Nrf2 cascades. J Pineal Res 50(2):124–131
28. Joshi RP, Negi G, Kumar A, Pawar YB, Munjal B, Bansal AK, Sharma SS (2013) SNEDDS curcumin formulation leads to enhanced protection from pain and functional deficits associated with diabetic neuropathy: an insight into its mechanism for neuroprotection. Nanomed: Nanotechnol, Biol Med 9(6):776–785
29. Phan C-W, David P, Naidu M, Wong K-H, Sabaratnam V (2013) Neurite outgrowth stimulatory effects of culinary-medicinal mushrooms and their toxicity assessment using differentiating Neuro-2a and embryonic fibroblast BALB/3T3. BMC Complement Altern Med 13(1):261–270
30. Bass DA, Parce JW, Dechatelet LR, Szejda P, Seeds MC, Thomas M (1983) Flow cytometric studies of oxidative product formation by neutrophils: a graded response to membrane stimulation. J Immunol 130(4):1910–1917
31. Mukhopadhyay P, Rajesh M, Yoshihiro K, Hasko G, Pacher P (2007) Simple quantitative detection of mitochondrial superoxide production in live cells. Biochem Biophys Res Commun 358(1):203–208
32. Massicot F, Hache G, David L, Chen D, Leuxe C, Garnier-Legrand L, Rat P, Laprevote O et al (2013) P2X7 cell death receptor activation and mitochondrial impairment in oxaliplatin-induced apoptosis and neuronal injury: cellular mechanisms and in vivo approach. PLoS One 8(6), e66830
33. Yates D (2013) Cell biology of the neuron: fuelling transport. Nat Rev Neurosci 14(3):156–157
34. Gustafsson H, Söderdahl T, Jönsson G, Bratteng JO, Forsby A (2004) Insulin-like growth factor type 1 prevents hyperglycemia-induced uncoupling protein 3 down-regulation and oxidative stress. J Neurosci Res 77(2):285–291
35. Belliveau DJ, Bani-Yaghoub M, McGirr B, Naus CC, Rushlow WJ (2006) Enhanced neurite outgrowth in PC12 cells mediated by connexin hemichannels and ATP. J Biol Chem 281(30):20920–20931
36. D'Ambrosi N, Murra B, Cavaliere F, Amadio S, Bernardi G, Burnstock G, Volonte C (2001) Interaction between ATP and nerve growth factor signalling in the survival and neuritic outgrowth from PC12 cells. Neuroscience 108(3):527–534
37. Obrosova IG (2009) Diabetes and the peripheral nerve. Biochim Biophys Acta (BBA)-Mol Basis Dis 1792(10):931–940
38. Ellis A, Bennett D (2013) Neuroinflammation and the generation of neuropathic pain. Br J Anaesth 111(1):26–37
39. Pop-Busui R, Marinescu V, Van Huysen C, Li F, Sullivan K, Greene DA, Larkin D, Stevens MJ (2002) Dissection of metabolic, vascular, and nerve conduction interrelationships in experimental diabetic neuropathy by cyclooxygenase inhibition and acetyl-L-carnitine administration. Diabetes 51(8):2619–2628
40. Soriano FG, Virág L, Jagtap P, Szabó É, Mabley JG, Liaudet L, Marton A, Hoyt DG et al (2001) Diabetic endothelial dysfunction: the role of poly (ADP-ribose) polymerase activation. Nat Med 7(1):108–113
41. Schulz E, Schuhmacher S, Münzel T (2009) When metabolism rules perfusion AMPK-mediated endothelial nitric oxide synthase activation. Circ Res 104(4):422–424
42. Yerra VG, Negi G, Sharma SS, Kumar A (2013) Potential therapeutic effects of the simultaneous targeting of the Nrf2 and NF-κB pathways in diabetic neuropathy. Redox Biol 1(1):394–397
43. Salminen A, Hyttinen JM, Kaarniranta K (2011) AMP-activated protein kinase inhibits NF-κB signaling and inflammation: impact on healthspan and lifespan. J Mol Med 89(7):667–676
44. Feldman EL (2003) Oxidative stress and diabetic neuropathy: a new understanding of an old problem. J Clin Investig 111(4):431
45. Sandireddy R, Yerra VG, Areti A, Komirishetty P, Kumar A (2014) Neuroinflammation and oxidative stress in diabetic neuropathy: futuristic strategies based on these targets. Int J Endocrinol
46. Kumar A, Yerra VG, Malik RA (2015) Comment on Sharma. Mitochondrial hormesis and diabetic complications. Diabetes 64:663–672, Diabetes 64 (9):e32-e33
47. Tomlinson DR, Gardiner NJ (2008) Glucose neurotoxicity. Nat Rev Neurosci 9(1):36–45
48. Uittenbogaard M, Chiaramello A (2014) Mitochondrial biogenesis: a therapeutic target for neurodevelopmental disorders and neurodegenerative diseases. Curr Pharm Des 20(35):5574–5593
49. St-Pierre J, Drori S, Uldry M, Silvaggi JM, Rhee J, Jäger S, Handschin C, Zheng K et al (2006) Suppression of reactive oxygen species and neurodegeneration by the PGC-1 transcriptional coactivators. Cell 127(2):397–408
50. Calkins MJ, Manczak M, Mao P, Shirendeb U, Reddy PH (2011) Impaired mitochondrial biogenesis, defective axonal transport of mitochondria, abnormal mitochondrial dynamics and synaptic degeneration in a mouse model of Alzheimer's disease. Hum Mol Genet 20(23):4515–4529
51. Chandrasekaran K, Muragundla A, Inoue T, Choi J, Chen C, Ide T, Russell JW (2015) Mitochondrial transcription factor A regulation of mitochondrial degeneration in experimental diabetic neuropathy. Am J Physiol-Endocrinol Metab 309(2):E132–141
52. Banerjee R, Beal MF, Thomas B (2010) Autophagy in neurodegenerative disorders: pathogenic roles and therapeutic implications. Trends Neurosci 33(12):541–549
53. Glick D, Barth S, Macleod KF (2010) Autophagy: cellular and molecular mechanisms. J Pathol 221(1):3–12
54. Yerra VG, Gundu C, Bachewal P, Kumar A (2015) Autophagy: the missing link in diabetic neuropathy? Med Hypotheses 86:120–126